

# Experimental demonstration of RSOA-based WDM PON with PPM-encoded downstream signals

Lei Liu (刘磊), Min Zhang (张民), Mingtao Liu (刘明涛), and Xiaopin Zhang (张小频)

State Key Laboratory of IPOC, Beijing University of Posts and Telecommunications, Beijing 100876, China

\*Corresponding author: liuleibupt@bupt.edu.cn

Received December 21, 2011; accepted February 13, 2012; posted online April 12, 2012

Pulse position modulation (PPM) is introduced downstream of the reflective semiconductor optical amplifier (RSOA)-based single-fiber full-duplex bidirectional wavelength division multiplex passive optical network (WDM PON) to suppress the interference brought by the remodulation effect in the RSOA, Rayleigh backscattering, and reflection of the connection devices. In addition, because of the power-efficient characteristic of the PPM-encoded signals, the power budget shows clear improvement. As the experimental tests indicate, with  $\sim 6$  dB extinction ratio (ER) in the downstream signal, the receiving sensitivity of the PPM-encoded channel is  $\sim 2.6$  and  $\sim 3$  dB higher than that of the NRZ (Non-return to zero)-encoded channel in the downlink and uplink, respectively.

OCIS codes: 060.0060, 100.6640, 210.4770, 180.1790.

doi: 10.3788/COL201210.070608.

Because of good amplification and modulation characteristics, the reflective semiconductor optical amplifier (RSOA)-based colorless optical network unit (ONU) is a promising candidate for deploying wavelength division multiplex passive optical networks (WDM PONs)<sup>[1–3]</sup>. RSOA-based full-duplex bidirectional WDM PON has two key limitations. First, the RSOA is a bandwidth-limited device. Without signal processing, the modulation bandwidth cannot exceed 2.5 GHz. Second, RSOA-assisted ONU is vulnerable to interference brought by the remodulation effect, Rayleigh backscattering (RB), and reflections<sup>[4–6]</sup>. Facing these problems, many schemes have been reported recently. With the help of electrical equalization and high-efficiency forward error correction (FEC)<sup>[7–10]</sup>, the modulating bandwidth of RSOA can be enlarged to beyond 10 GHz, which means it may be a promising prospect for large-scale application. By using frequency-shift keying (FSK) modulation<sup>[11,12]</sup> or optical carrier suppressed (OCS) modulation<sup>[13–15]</sup> with a Mach-Zehnder modulator (MZM) to shift the frequency between downstream and upstream signals, the interference can be suppressed.

In this letter, pulse position modulation (PPM) is introduced into the downlink to suppress the interference and reduce the power budget<sup>[16,17]</sup>. The PPM-encoded signals, with very different the frequency distribution from the non-return to zero (NRZ)-encoded signals, have less impact on the NRZ-encoded signal, which significantly improves the upstream signal performance. In addition, PPM is a power-efficient modulation scheme that aids long-reach network realization. As a result, we could substantially improve the power budget of the RSOA-assisted WDM PON by using PPM instead of on-off keying (OOK) in the downlink.

The principle of PPM-encoded signal generation is shown in Table 1. In PPM, the symbol duration is cut into  $M$  time chips, and the optical pulse occupies one of the  $M$  chips. As a result, for any  $M$  greater than 2, PPM requires less optical power than OOK. However, the spectrum efficiency of MPPM is much lower than that of NRZ. Under the same symbol rate, for PPM-encoded

channels, the required bandwidth is  $\log_2 M$  times larger than that for NRZ channels. To balance the spectrum efficiency and the power budget, digital PPM (DPIM) and differential PPM (DPPM) are utilized. DPIM and DPPM can provide much higher spectrum efficiency than quantized PPM (QPPM) because all the unused timeslots from within each symbol are erased. As Table 1 shown, a symbol that encodes  $M$  bits of data is represented by a pulse of constant power in one slot followed by  $k$  slots of zero power, where  $1 < k < L$  and  $L = 2M$ .

The spectral differences between the PPM and NRZ signals are numerical simulated in Fig. 1. The frequency distribution of the PPM-encoded signals does not concentrate in the zero frequency because only one bit exists in every timeslot in the PPM-encoded signals. As a result, the PPM-encoded signals have less interference on the upstream NRZ-encoded signals and the performance of the upstream signal be improved.

Figure 2 depicts the experimental setup of the full-duplex bidirectional communication system with an optical line terminal (OLT) and ONU. In the OLT, the downstream optical signals were obtained by modulating a decision feedback laser diode (DFB-LD) operating at 1549.32 nm with a dual-driver MZM (DDMZM). The multiple encoded electrical signals driving the DDMZM were generated by a pulse position generator (PPG<sub>1</sub>) (MP1800A). A polarization controller (PC) was placed before the DDMZM to emit the maximized optical power. After an optical circulator (CIR) and a 1×4 multiplexer (MUX), the signal was launched over 30 km of a single-mode fiber (SMF) with 6.4 dB total insert

**Table 1. Coding Principle of the PPM and NRZ Signals**

Original	NRZ	QPPM	DPPM	DPIM
00	00	0001	1	1
01	01	0010	10	01
10	10	0100	100	001
11	11	1000	1000	0001

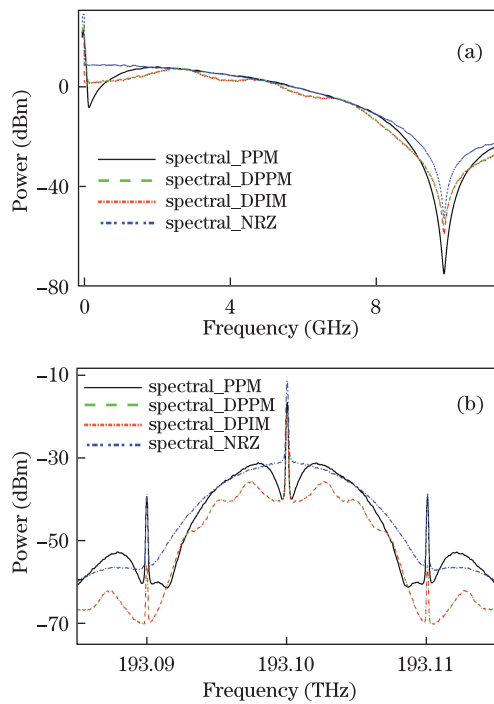


Fig. 1. (a) Electrical and (b) optical spectra of the downstream signal.

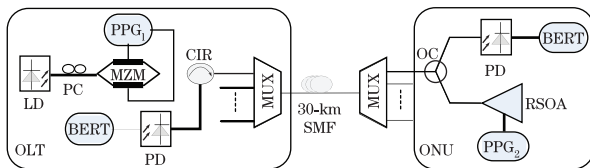


Fig. 2. Experimental setup of the RSOA-based full-duplex colorless ONU system. BERT: bit error detector.

loss (IL). A demultiplexer (DEMUX) was used to filter the downstream signal and sent it to the desired ONU.

At the desired ONU, the downstream signal was divided into two parts with a ratio of 50:50 at the optical coupler (OC). The signal at the lower arm was used to excite the RSOA, serving as the upstream carrier, whereas the signal at the upper arm was detected by the photodetector (PD). In this test, a 10-GHz bandwidth PIN was used as the PD with a receiving sensitivity of  $-19$  dBm. The RSOA was a commercially available device (CIP SOA-RL-OEC-1 550) with 1.5-GHz modulation bandwidth and 24-dB small signal gain at 50-mA bias current. The RSOA was biased at 70 mA (in order to provide a higher gain and balance the line loss) and driven with a 4-V peak-to-peak NRZ-encoded signal (a 2.5-Gb/s,  $2^{11}-1$ -long pseudo-random binary sequence (PRBS) generated by a PPG<sub>2</sub> (MP1703C)). Both the downstream and upstream signals were detected by a digital sampling oscilloscope and processed off-line.

The eye diagrams of both the downstream and upstream signals are shown in Fig. 3. All the eye diagrams were taken after the 30-km fiber transmission with the same received optical power at  $-10$  dBm. In order to analyze the downstream effect on the upstream signal, the

same modulation index was used in the downstream (Fig. 3). The PPM-coded signal downstream signal exhibited better performance than the NRZ-coded signal. In addition, the upstream signal had less influence in the PPM-encoded channel than that in the NRZ-encoded channel.

The system performance was characterized by BER measurements, as reported in Fig. 3. The bit rates of all the encoded downstream signals were set as 10 Gb/s. The modulation index, which is defined as the ratio of the bias voltage to the  $V_{\pi}$ , was fixed at 55% with the same signal amplitude of 1.5 V. The extinction ratio (ER) of the downstream optical signals was  $\sim 6$  dB. Nevertheless, the quantity of the information carried in the downlink was different. According to the coding principle of the PPM signals, with the same bit rate, the QPPM signals contained only 50% of the NRZ signals. For DPPM and DPIM, the data size was approximately 75% of the NRZ signals.

In this scenario, as Fig. 4 indicates, the power sensitivity of the PPM-encoded signal was  $\sim 2.6$  dBm lower than that of the NRZ signals. For the DPPM or DPIM signal, the improvement of the power sensitivity was  $\sim 1.5$  dBm.

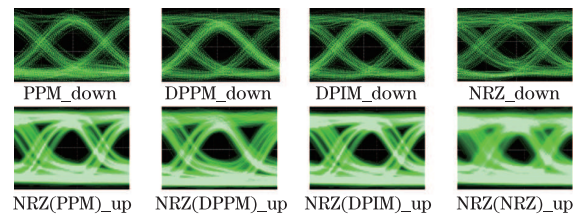


Fig. 3. Eyediagrams of the downstream signals and upstream signals.

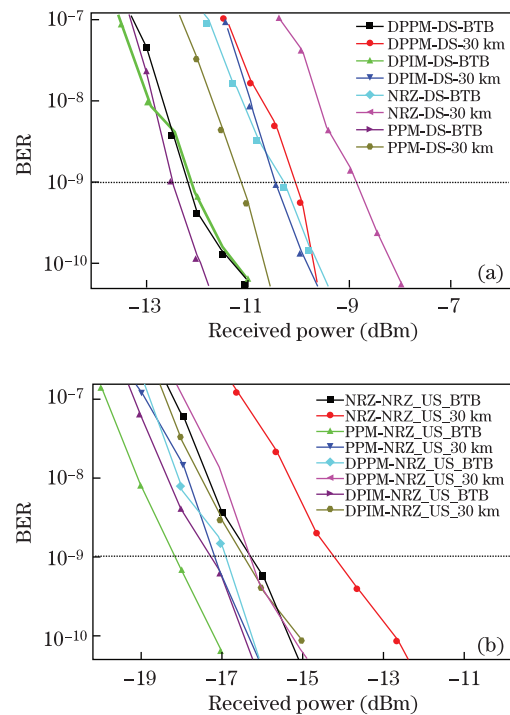


Fig. 4 BER curves versus received power employing PPM-, DPPM-, DPIM-, and NRZ-coded downstream signal, BER curves of the (a) downstream and (b) upstream signals.

Increasing ER of the downstream signal raises the improvement correspondingly. As ER approaches infinity, the improvement of the power sensitivity would equal 6 dB for the QPPM signals. However the rise of the ER of the downstream signals would degenerate the upstream signal. Thus, the trade-off of the downstream and upstream signals should be considered when setting up the system.

For the upstream signal, the PPM signals have less effect on the upstream signal. As a result, upstream signal remodulating the PPM signals showed better performance than the NRZ ones. The power sensitivity of the upstream signal with PPM downstream signal was 3 dB, showing an improvement over the NRZ signal.

Because ER is dominated by MI, the influence of ER on the downstream signal and upstream signal was analyzed by varying the modulation index from 45% to 65%. The BER curve versus modulation index is given in Fig. 5. Because modulation index affects not only the ER of the downstream, but also the injected power of the RSOA, when modulation index increases, the injected power becomes reduced and degenerates the upstream signal performance. As a result, the ranges of modulation index for the error-free transmission ( $BER=10^{-9}$ ) in both the downlink and uplink were much larger than in the test ones. As shown in Fig. 5, the threshold modulation index es should be  $\sim 53\%$ ,  $\sim 57.5\%$ , and  $\sim 61\%$  for the NRZ-NRZ, DPIM/DPPM-NRZ, and QPPM-NRZ systems to achieve the error-free transmission.

The bias current and the injected optical power of the RSOA are the main parameters defining the working statement of the RSOA-based system. The influence of the optical injected power on the RSOA-modulated upstream signal is given in Fig. 6. For simplification, only QPPM- and NRZ-encoded signals were used in the

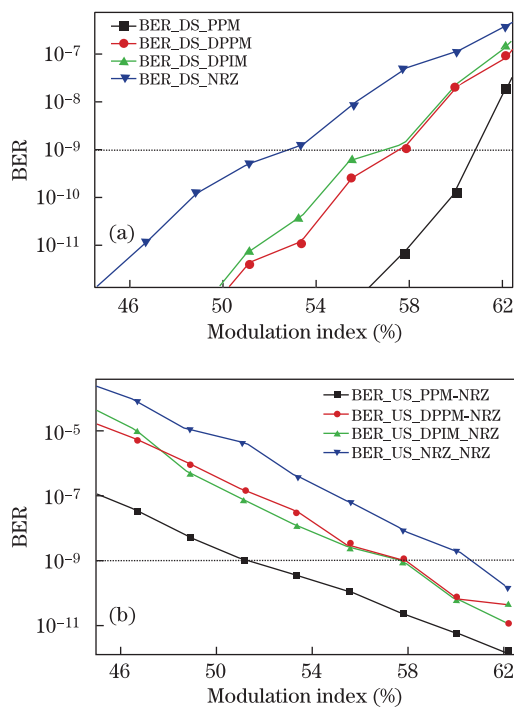


Fig. 5. BER curves versus modulation index; (a) BER curves of the downstream and (b) upstream signals.

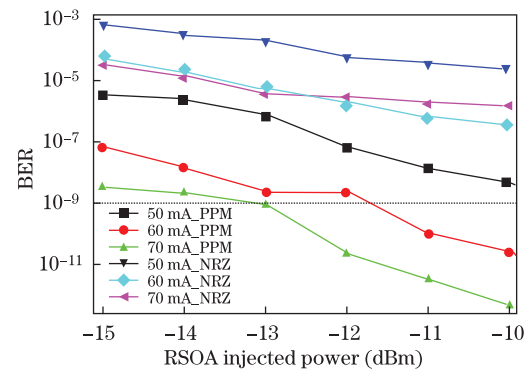


Fig. 6. Upstream signal BER curve employing the PPM- and NRZ-coded downstream signals versus injected optical power into the RSOA.

downstream. As shown in Fig. 6, the performance of the upstream signal was optimized by increasing the bias current and the injected optical power. Higher optical power and bias current would increase the saturation degree, and then suppress the downstream signal and increase the ER of the upstream signal.

In conclusion, we evaluate the performance of the RSOA-based WDM PON with the PPM-encoded downstream signals. QPPM-encoded downstream signals can effectively suppress the interference between the downstream signals and upstream signals and improve the optical receiving sensitivity; however, spectrum efficiency is only 50% of that of the NRZ-encoded signals. In order to balance the spectrum efficiency and the power sensitivity, the DPPM and DPIM are introduced into the downlink. Compared with the QPPM-encoded signal, the spectrum efficiency of the DPPM- and DPIM-encoded signals improved by approximately 25%, and the power sensitivity is reduced by approximately  $\sim 1$  dB.

This work was supported by the National Natural Science Foundation of China (No. 61072008), the National "863" Project of China (No. 2009AA01z255), the National "111" Project of China (No. B07005), the Beijing New Star Programme of Science and Technologies (No. 2007A048), the Fundamental Research Funds for Central Universities (Nos. 2009GYBZ and 2009RC0401), and the Program for Excellent Talents in BUPT.

## References

1. G. Berrettini, G. Meloni, L. Giorgi, F. Ponzini, F. Cavaliere, P. Ghiggino, L. Poti, and A. Bogoni, *IEEE Photon. Technol. Lett.* **21**, 453 (2009).
2. A. Bogoni, *IEEE J. Sel. Top. Quantum Electron.* **17**, 472 (2011).
3. E. T. Lopez, J. A. Lazaro, C. Arellano, V. Polo, and J. Prat, *IEEE Photon. Technol. Lett.* **22**, 97 (2010).
4. S. Moon, H. Lee, and C. Lee, in *Proceedings of CLEO'2011 CFH1* (2011).
5. H. Hu and H. Anis, *IEEE J. Lightwave Technol.* **26**, 870 (2008).
6. P. Li, J. Xu, and L. Chen, in *Proceedings of OECC'2011* 15 (2011).
7. Q. Guo, A. V. Tran, and C. Chae, *IEEE Photon. Technol. Lett.* **23**, 1442 (2011).

8. H. Kim, in *Proceedings of OFC'2011* OMP8 (2011).
9. B. Schrenk, G. de Valicourt, M. Omella, J. A. Lazaro, R. Brenot, and J. Prat, *IEEE Photon. Technol. Lett.* **22**, 392 (2010).
10. K. Y. Cho, J. H. Chang, B. S. Choi, Y. Takushima, and Y. C. Chung, in *Proceedings of OFC'2011* OMP2 (2011).
11. B. Schrenk, G. de Valicourt, J. A. Lazaro, and J. Prat, in *Proceedings of OFC'2011* JWA79 (2011).
12. J. Prat, C. Arellano, V. Polo, and J. Lazaro, in *Proceedings of ECOC'2006* 531 (2006).
13. C. W. Chow, G. Talli, A. D. Ellis, and P. D. Townsend, *Opt. Express* **16**, 1860 (2008).
14. T. T. Pham, H. Kim, Y. Won, and S. Han, in *Proceedings of OFC'2009* OThA2 (2009).
15. L. Liu, M. Zhang, M. Liu, X. Zhang, and P. Ye, *Chin. Opt. Lett.* **9**, 020606 (2011).
16. F. Xu, M. Khalighi, and S. Bourennane, *J. Opt. Commun. Netw.* **1**, 404 (2009).
17. N. Azzam, M. H. Aly, and A. K. AboutiSeoud, in *Proceedings of NRSC'2009* C10 (2009).